Bioorganic Chemistry 82 (2019) 17–25

Contents lists available at ScienceDirect

Bioorganic Chemistry

journal homepage: www.elsevier.com/locate/bioorg

How the surface functionalized nanoparticles affect conformation and activity of proteins: Exploring through protein-nanoparticle interactions

Sathish Dyawanapelly[a,b], Pihu Mehrotra[b], Goutam Ghosh[c], Dhanashree D Jagtap[d], Prajakta Dandekar[b,*], Ratnesh Jain[a,*]

[a] Department of Chemical Engineering, Institute of Chemical Technology, Matunga, Mumbai 400019, India
[b] Department of Pharmaceutical Sciences and Technology, Institute of Chemical Technology, NP Marg, Matunga, Mumbai 400019, India
[c] UGC-DAE CSR, Trombay, Mumbai 400085, India
[d] Division of Structural Biology, National Institute for Research in Reproductive Health, Parel, Mumbai 400012, India

ARTICLE INFO

Keywords:
Counterion
Lysozyme
Low molecular weight chitosan
Reverse-charge-parity counterion
Protein-nanoparticle electrostatics interaction

ABSTRACT

To understand the effect of counter ions (Na^+) on the secondary conformation and functionality of the lysozyme, we have studied the interaction of lysozyme with counterion associated iron oxide nanoparticles (IONPs). The investigation was carried out at pH 7.4 and 9.0, with three different types of NPs, namely, bare IONPs, low molecular weight chitosan modified IONPs (LMWC-IONPs) and the counterion (Na^+) associated sodium tripolyphosphate IONPs (STP-LMWC-IONPs) and confirmed by using various spectroscopy techniques. The difference in UV–vis absorbance (ΔA) between native and STP-LMWC-IONPs interacted hen egg white lysozyme (HEWL) was greater than that between native and NPs interacted HEWL at pH 9.0 compared with pH 7.4. Furthermore, STP-LMWC-IONPs exhibited quenching effect on lysozyme fluorescence spectrum at pH 9.0 due to binding of Na^+ counterions to the protein, confirming denaturation of the latter. After HEWL interaction with STP-LMWC-IONPs (pH 9.0), CD spectra revealed a conformational change in the secondary structure of HEWL. Also, counterion induced lysozyme inactivation, due to interaction with nanoparticles at pH 9.0, was confirmed by enzymatic activity assay involving lysis of *Micrococcus lysodeikticus*. In conclusion, pH 9.0 was observed to be a more favorable condition, compared to pH 7.4, for the strongest electrostatic interaction between lysozyme and NPs. We postulate that the counterions in nanoparticle surface-coating can ameliorate protein misfolding or unfolding and also prevent their aggregation and, therefore, can be considered as a powerful and potential therapeutic strategy to treat incurable neurodegenerative disorders.

1. Introduction

Nanoparticles (NPs) have attracted substantial attention in the development of new diagnostic and therapeutic strategies against many diseases; due to their unique and attractive properties such large surface area-to-volume ratio, size, surface charge, and bio-compatibility. When used for biomedical applications, NPs can interact with proteins inside the body and induce significant perturbations in their structure and functions, resulting in misfolded protein fibrils. In recent years, misfolding of proteins mediated by NPs has shown great promise for alleviating many human amyloidogenic diseases. Many research groups have, therefore, extensively studied the interaction of amyloid protein fibrils with different types of NPs that have exhibited potential for the therapy of neurodegenerative disorders [1]. In neurodegenerative diseases, protein fibrils accumulate in various parts of the body that exerts toxicity by interrupting intracellular transport, overwhelming protein degradation mechanisms, and/or altering vital cellular activities. *In vitro* and *in vivo*, protein interaction behavior can be regulated by modifying physicochemical properties including ionic strength, pH, temperature and other several factors such as hydrophobicity, the secondary structure of proteins, the activity of chaperons, inhibitors and also size and shape of NPs [2–4]. However, NPs possess an enormous surface area and the interaction of NPs with proteins can affect both conformation and activity of the protein.

Amongst the varied NP systems, magnetic NPs have been extensively employed in diverse biomedical applications including, diagnosis, biomedical imaging, drug delivery, as biosensors and for cancer hyperthermia [5]. Moreover, the safety and efficacy of these nanoparticles can be suitably tailored using appropriate ligands, e.g., polymers, lipids, detergents, small biomolecules [6]. Despite their huge

* Corresponding authors.
E-mail addresses: pd.jain@ictmumbai.edu.in (P. Dandekar), rd.jain@ictmumbai.edu.in (R. Jain).

https://doi.org/10.1016/j.bioorg.2018.09.020
Received 23 July 2018; Received in revised form 9 September 2018; Accepted 11 September 2018
Available online 15 September 2018
0045-2068/

potential, the interaction of surface modified magnetic-nanoparticles with proteins has not been widely explored. This is especially important because NP surfaces can specifically interact with misfolded proteins and have the capability to interfere with the fibrillation process [7] which is a hallmark of many neurodegenerative disorders [8].

For this purpose, we have used biocompatible low molecular weight chitosan (LMWC) polymer for surface modification of IONPs, which can improve the interactions between NPs and cells [9,10]. In pH 9.0, selective binding of LMWC-IONPs was observed with protein, which is in fair agreement with earlier results on the reverse-charge-parity model. In addition, *in-vitro* cell toxicity study confirmed that LMWC-IONPs are safe in mammalian cell lines [9]. The investigation employed lysozyme as an amyloidogenic model protein because of its homology to human lysozyme [11]. It is also the most extensively used model protein for studying protein-nanoparticle interactions [9]. It is abundantly found in biological fluids such as tears, saliva, serum or urine.

The reason for lysozyme being extensively used as a model protein for folding and aggregation mechanism is the abundant information available on its 3D structure, aggregation mechanisms and folding/unfolding process [12]. Lysozyme or hen egg white lysozyme (HEWL) is also a well-known enzyme that specifically degrades the microbial cell wall by hydrolysis of β-(1 → 4)-glycosidic bonds between *N-acetyl muramic acid* and *N-acetyl glucosamine* in peptidoglycan sugar backbone. The enzymatic activity of lysozyme presents a convenient tool to determine any changes in activity and hence can be suitably used to study the structure of HEWL upon NPs interaction [13]. Owing to these properties, lysozyme has been selected as a model protein to study surface modified magnetic interactions.

In one study, Ghosh et al. have proposed *protein-nanoparticle-RPC*-counterion model and have demonstrated the electrostatic interaction between negative surface NPs and positive surface HEWL [14]. Recently, we have published "protein-nanoparticle electrostatic interactions of surface-modified iron oxide nanoparticles (LMWC-IONP) with lysozyme" at various pH ranges 3.0–12.0 [9]. Our findings demonstrated that pH 9, which is favorable for the electrostatic protein-nanoparticle interaction. In addition, we have confirmed biocompatibility of NPs for safe biomedical use. The present work is an extension of an earlier study on "effect of counterion functionalized biocompatible LMWC-IONPs on activity and conformation of lysozyme". In this study, we have applied our previously gained knowledge of protein-nanoparticle electrostatic interaction. Here, we have employed sodium tripolyphosphate (STP), which contains Na^+ as a counterion. STP plays a dual role in this study, on the one hand, as counterion agent and, on the other hand, as cross-linking agent i.e., negatively charged phosphate groups of STP cross-links with amino groups of chitosan (shown Fig. 1A). Using this model, we predict the results of competitive binding of three different NPs to lysozyme, as a function of pH. Also, electrostatic interactions between protein and NPs were investigated using zeta potential measurements. Further, fluorescence quenching and conformational changes in protein secondary structure, before and after interaction with NPs, were investigated with the help of fluorescence spectroscopy and circular dichroism (CD). In addition, an enzymatic assay was executed to the elucidate activity of interacted lysozyme using *Micrococcus lysodeikticus* cells, which also supports the CD studies.

2. Materials and methods

2.1. Materials

Hen egg white lysozyme (Lyophilized powder, chicken egg white, ≥ 90%), sodium tripolyphosphate (85%, M_W = 367.86 g/mol), $FeCl_3{\cdot}6H_2O$ (97% purity), $FeCl_2{\cdot}4H_2O$ (99% purity), NH_4OH (30%) and lyophilized cells of *M. lysodeikticus* (A.T.C.C. 4698) were procured from Sigma-Aldrich, St. Louis, USA. LMWC (M_W ~ 20KDa) was gift product from Amicogen Co., Korea. Fresh 10 mM Tris buffer and deionized water (DIW) is used for the preparation of stock solutions.

2.2. Synthesis and surface modification of IONPs

IONPs was synthesized from chemical co-precipitation technique using aqueous alkaline (30% NH_4OH) solution [15]. The synthesis procedure has been elaborated in our previous manuscript [9]. The resulting IONPs was separated by strong magnet and followed by alternately washing with DIW until neutral pH value is achieved in the supernatant. Then, the surface of IONPs is coated with positively charged-LMWC polymer using a previously reported method [9]. The separated LMWC-IONPs were washed alternately with DIW to remove free LMWC. The surface of cationic LMWC-IONPs was further grafted with anionic STP molecules, containing Na^+ counterions (Fig. 1A). In brief, dried LMWC-IONPs was added in STP solution and sonicated for 2 h [15]. STP-LMWC-IONPs were then separated by the magnet at the bottom of the container. The supernatant was decanted and the black precipitate of NPs was washed several times with deionized water to remove unbound STP molecules. The samples were dried at 25 °C until further use.

2.3. Surface characterization of NPs by FT-IR spectrophotometer

Surface modification of IONPs was assessed using FTIR spectrophotometer (IR affinity-1, Shimadzu, Japan), using KBr-potassium bromide pellet method. About 5 mg of NPs was mixed with 100 mg of dried KBr and then pelletized at 10,000–14,000 psi using a hydraulic press. The characteristic peaks for all samples were recorded in the wave number range of 400–4000 cm^{-1}, with a resolution of 1 cm^{-1}.

2.4. Surface characterization of NPs by zeta potential measurements

The influence of pH on the surface charge of NPs is extremely important while investigating protein-nanoparticle electrostatic interactions. Zeta potential of three NPs and native lysozyme was analyzed at pH 7.4 and 9.0 with dynamic light scattering analysis (DLS; Malvern Zetasizer Nano ZSP), which are used as controls for protein interaction studies. Similarly, all zeta potential values were obtained in triplicate experiments.

2.5. Incubation of proteins with nanoparticles

The surface charge of both NPs and HEWL in the range of pH 3.0–12.0 have been reported in our earlier publication [9]. Based on the earlier results of *reverse charge parity counterion (RCPC) model*, here, we have selected two pH values 7.4 and 9.0 to assess the electrostatic interactions between negative surface charge counterion-associated NPs and positive surface charge protein. Fig. 1B depicts zeta potential values for lysozyme and STP-LMWC-IONPs in the range of pH 3.0–12.0. Clearly, pH 7.4 and 9.0 were observed to be suitable for studying the protein-nanoparticle RCPC interaction, due to the presence of opposite charges at this pH. Here, lysozyme solution (1 mg/mL) was freshly prepared in 10 mM Tris buffer (at pH 7.4 and 9.0). Thereafter, dry powder (concentration: 1 mg/mL) of each nanoparticulate system (IONPs, LMWC-IONPs, and STP-LMWC-IONPs) was separately dispersed into the protein solution, at 4 °C for 48 h. After 48 h incubation, we have collected supernatant (NPs interacted lysozyme) from the samples by separating magnetic NPs using a strong magnet. Then, interacted-lysozyme is used for further analysis including, zeta potential, UV–visible, fluorescence and CD spectroscopy.

2.6. Protein-nanoparticle electrostatic interaction by zeta potential measurements

The protein-nanoparticle electrostatic interaction can be determined by variation in their surface charges, which was confirmed by measuring the zeta potential of both, '*interacted lysozyme*' and '*lysozyme adsorbed nanoparticles*' [14]. All zeta potential measurements were

recorded in triplicate using Zetasizer Nano ZSP instrument, at 25 °C.

2.7. Protein-nanoparticle interactions using spectroscopic techniques

The UV–visible spectrum of 'native HEWL' and 'NPs interacted HEWL' was analyzed at far-UV 180–230 nm region and near-UV 240–300 nm region by using a DeNovix DS-11 UV–vis spectrophotometer. Difference in the absorbance (ΔA) spectra of '*native lysozyme'* and '*NPs-interacted lysozyme*' was determined by subtracting the absorbance of 'native lysozyme' from the absorbance of 'interacted lysozyme' over a range of 220–250 nm.

Further, counterion-induced fluorescence quenching of HEWL was explored using a SynergyH1 model fluorescence spectrophotometer USA, between 300 and 450 nm, at an excitation wavelength of 295 nm. Appropriate blanks corresponding to the buffer were subtracted to correct background fluorescence.

CD experiments were carried out to evaluate the counterion-induced change in the secondary conformation of lysozyme, using circular dichroism spectrometer, Jasco J-815, USA. All samples were measured over a range of 190–260 nm using a quartz cell with 1 mm path length at 25 °C. The CD spectra were subjected to baseline corrections. Each spectrum was the average of three successive scans (scan rate 100 nm/min) and determined using CD spectra deconvolution software CDNN 2.1, Germany.

2.8. Assay for enzymatic activity of lysozyme

Lysozyme assay was performed to understand the activity of native and interacted lysozyme using *M. lysodeikticus* cells. Lysozyme specifically degrades the microbial cell wall by hydrolyzing the β-(1 → 4) glycosidic bonds between *N*-acetyl muramic acid and *N*-acetyl glucosamine of peptidoglycan sugar backbone [16]. Briefly, *M. lysodeikticus* cell suspension (0.3 mg/mL) was freshly prepared in 66 mM KH_2PO_4 (pH 6.2). Activities of both 'native' and 'interacted' lysozyme were quantified by adding 50 µL of samples to 200 µL of cell suspension in a 96-well microplate. The change in optical density of cell suspension was recorded every 30 s and over a 4 min time period, at 450 nm, using Synergy H1 microplate reader, Bio-Tek Instruments, USA. The decrease in optical density of cell suspensions was regarded as an indication for the hydrolysis of cell wall, in turn reflecting the activity of lysozyme. The measurements were conducted in triplicate, at 25 °C.

Furthermore, change in turbidity of *M. lysodeikticus* cell suspension (lysozyme activity) in presence of lysozyme (native and interacted) was visualized by trypan blue staining method, under microscope (EVOS microscope, Life Technologies). Trypan blue is a colorimetric dye that stains dead cells with a distinctive blue color. After incubation with lysozyme (native and interacted), *M. lysodeikticus* cell suspension transferred on the hemocytometer and stained with trypan blue (0.4%), in 1:1 ratio and the turbidity (aggregates) was assessed using microscopy and all samples were captured in triplicate.

3. Results and discussion

3.1. Characterization of functionalized NPs by FT-IR

Three types of NPs were characterized by FT-IR spectra (Fig. 2) to confirm the surface modification of NPs. The FT-IR spectra exhibited a broad absorption band at 580 cm^{-1}, for all the three NPs, corresponding to the Fe—O bond vibration of IONPs [15]. The spectrum of LMWC-IONPs (Fig. 2B) showed a band at 1635 cm^{-1}, contributed by the primary amino group (—NH_2) of LMWC [17]. The broad and strong band at 3321 cm^{-1}, in this spectrum, may be attributed to overlapped stretching vibrations of the —OH and —NH functional groups of LMWC [17]. A new band observed at 1062 cm^{-1} (Fig. 2B) was attributed to

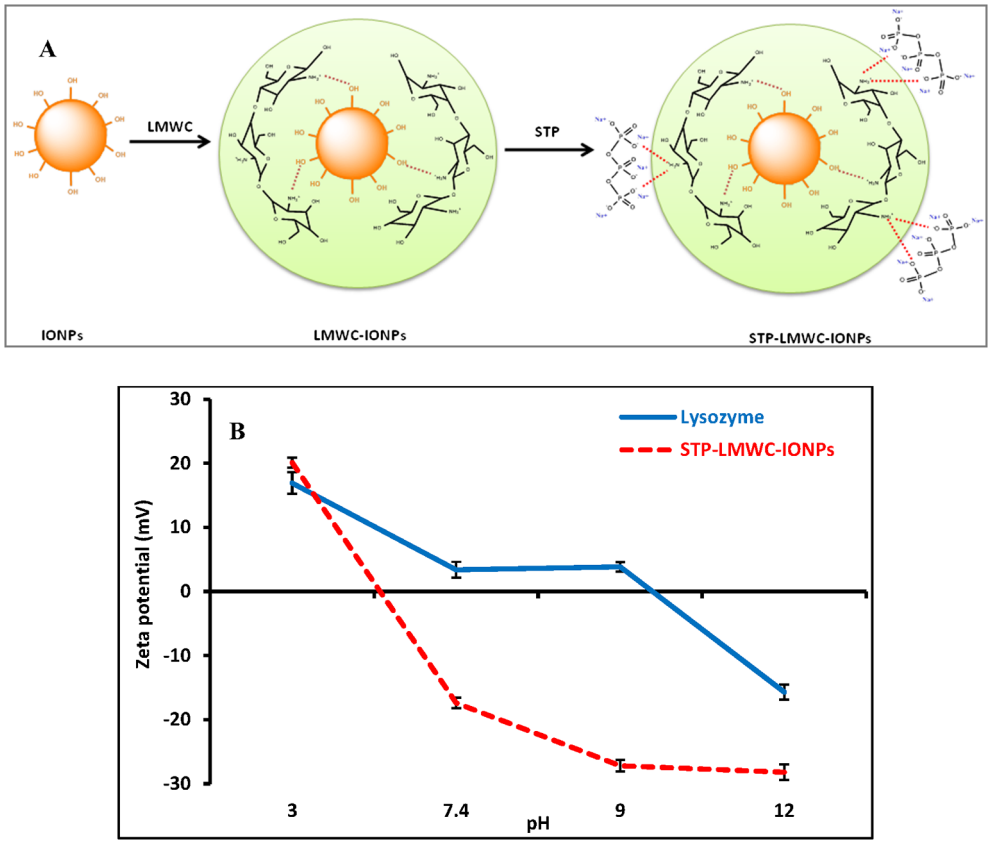

Fig. 1. (A) Schematic representation of surface functionalization of counterion associated STP-LMWC-IONPs. (B) pH-dependent zeta-potential analysis for lysozyme and STP-LMWC-IONPs in range of pH 3.0–12.0.

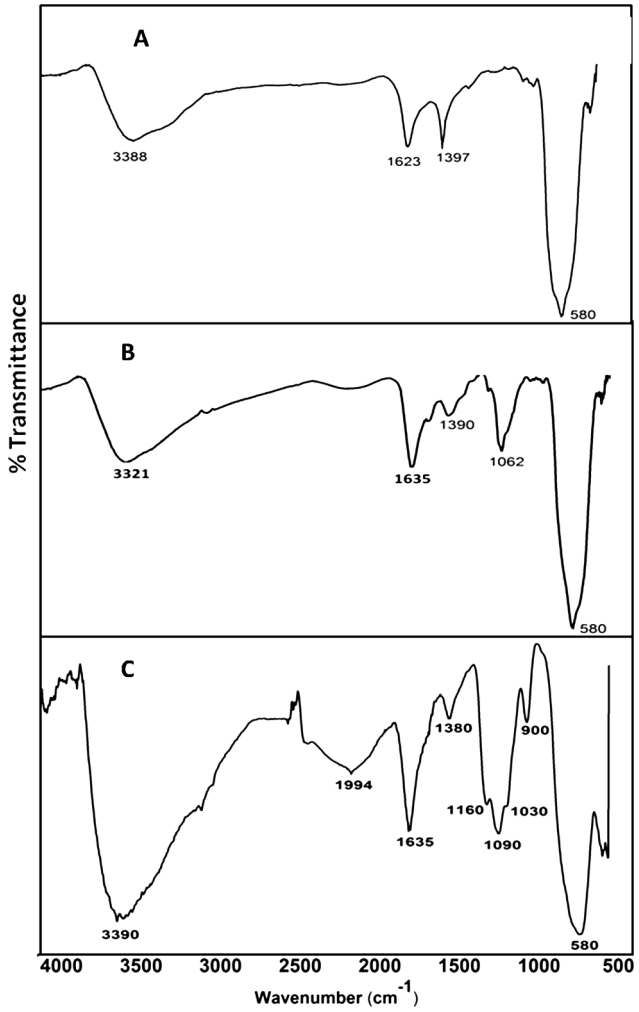

Fig. 2. FT-IR spectra of IONPs (A), LMWC-IONPs (B) and STP-LMWC-IONPs (C).

−CH−OH vibration of LMWC [18]. These results confirmed the presence of LMWC coating on IONPs.

In Fig. 2C, FT-IR (STP-LMWC-IONPs) spectra show the presence of characteristic absorption bands in the range of 1160–1030 cm^{-1} and at 900 cm^{-1}, corresponding to the P═O and P−O stretching modes, thus confirming the presence of STP on LMWC-IONPs [17]. These characteristic bands are absent in the IONPs and LMWC-IONPs spectra. Moreover, increased intensity of the band at 1635 cm^{-1}, from the spectrum of LMWC (Fig. 2C), indicated an ionic interaction between negatively charged phosphates ($-PO_4^{3-}$) groups of STP and amino ($-NH^{3+}$) groups of LMWC [19]. The absorption bands of STP, between 1160 cm^{-1} and 1030 cm^{-1}, were merged with new band observed in LMWC-IONPs at 1062 cm^{-1} (Fig. 2C). These results are also consistent with earlier reports [17,19] and confirmed the presence of STP on LMWC-IONPs.

3.2. Surface characterization of nanoparticles by zeta potential measurements

Fig. 3 shows the zeta potential of NPs at pH 7.4 and pH 9.0. At pH 7.4, upon surface modification of IONPs with LMWC, charge of IONPs (−4.16 ± 1.95 mV) was shifted to −1.68 ± 0.20 mV, and further changed to −17.40 ± 0.81 mV, after association with STP. Similarly at pH 9.0, upon LMWC coating surface charge of IONPs (−22.05 ± 4.45 mV) was shifted to −13.97 ± 2.65 mV, and then decreased to −27.20 ± 0.91 mV after association with STP. This large

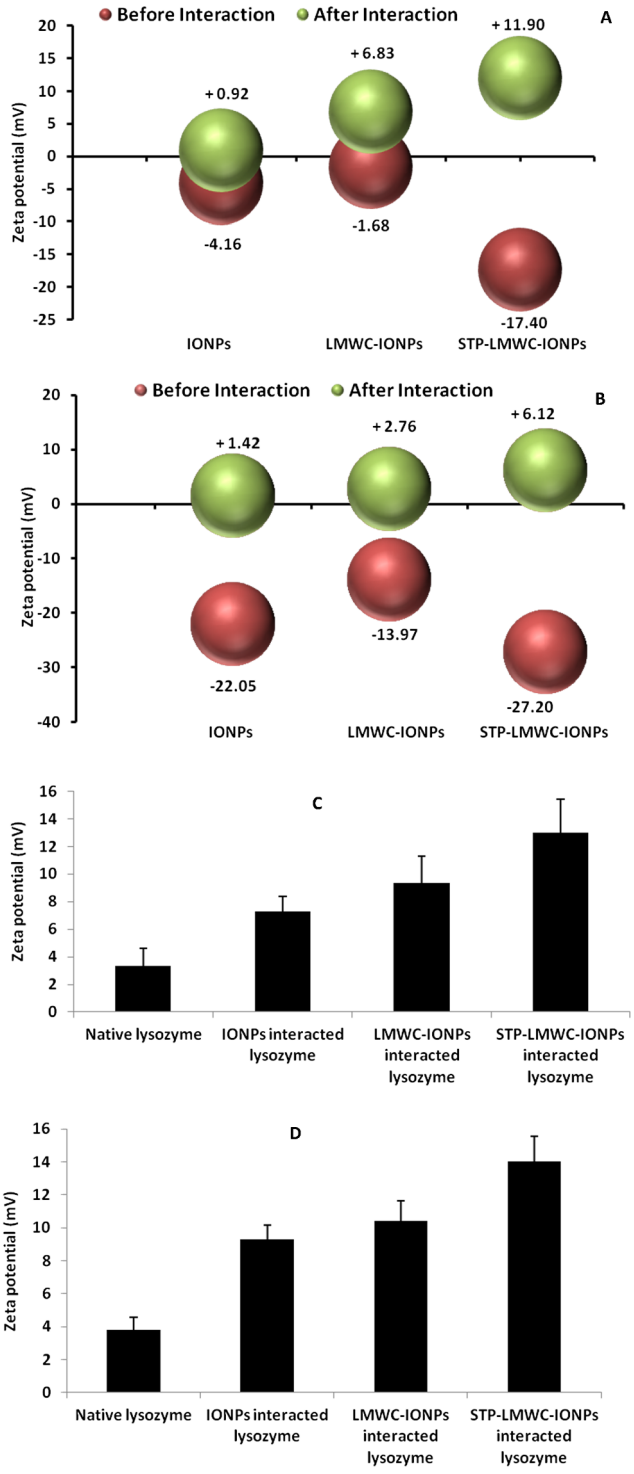

Fig. 3. Zeta potentials of protein adsorbed NPs at pH 7.4 (A) and 9.0 (B). Zeta potentials of NPs-interacted protein (present in supernatant) at pH 7.4 (C) and 9.0 (D).

negative charge on STP-LMWC-IONPs was attributed to the PO_4^{3-} groups of STP.

3.3. Investigating electrostatic interactions between protein and NPs using zeta potential measurements

In the earlier publication, we have reported pH-dependent surface charge analysis for both NPs and HEWL over the range of pH 3.0–12.0 [9]. In this study, we have measured the zeta potential of NPs before and

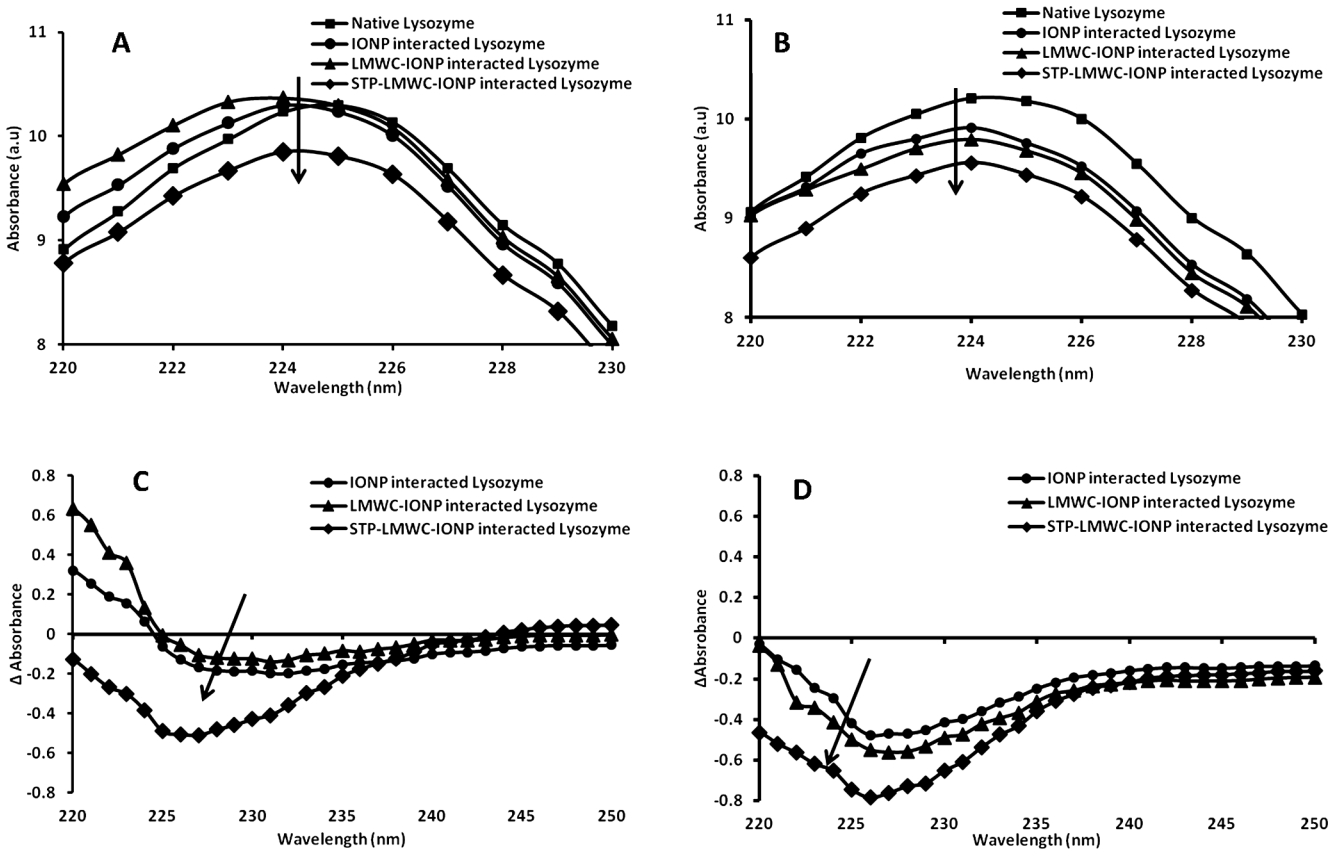

Fig. 4. UV–vis spectra of native-lysozyme and interacted-lysozyme with IONPs, LMWC-IONPs and STP-LMWC-IONPs at pH 7.4 (A), 9.0 (B). Difference in absorbance (ΔA) between native Lysozyme and NPs interacted Lysozyme in the far-UV region pH 7.4 (C) and 9.0 (D).

after interaction with lysozyme at pH 7.4 and 9.0 (Fig. 3A and B). Our results show that, upon electrostatic interaction with lysozyme, the zeta potential of negatively charged NPs turned positive, at both pH 7.4 and 9.0. After adsorption of lysozyme on nanoparticles, at pH 7.4, the zeta potential of IONPs (−4.16 ± 1.95 mV), LMWC-IONPs (−1.68 ± 0.20 mV) and STP-LMWC-IONPs (−17.40 ± 0.81 mV) increased to +0.92 ± 0.22 mV, +6.83 ± 0.33 mV and +11.90 ± 0.16 mV, respectively (see Fig. 3A and Table S1). Similarly, at pH 9.0, the zeta potential of IONPs (−22.05 ± 4.45 mV), LMWC-IONPs (−13.97 ± 2.65 mV) and STP-LMWC-IONPs (−27.20 ± 0.91 mV) increased to +1.42 ± 0.45 mV, +2.76 ± 0.21 mV and +6.12 ± 0.36 mV, respectively (see Fig. 3B). This was thought to be due to the binding of lysozyme (a positively charged protein) on the surface of NPs, which is in agreement with the RCPC interaction model [14]. These results were also consistent with surface charge results in our earlier reports [14,15]. This confirmed that the opposite charges of protein and nanomaterials can influence the protein-nanoparticle electrostatic interaction in the physiological conditions.

Furthermore, we recovered the 'interacted lysozyme' from the supernatant by separating lysozyme adsorbed NPs (Lys-NPs) using a strong magnet and measured the zeta potential of interacted lysozyme. After interaction with NPs, interacted lysozyme showed a drastic change of zeta potential from negative to positive values at both pH 7.4 (Fig. 3C) and pH 9.0 (Fig. 3D). This variation in zeta potential was consistent with all three types of NPs. Interestingly, STP-LMWC-IONP, upon interaction with lysozyme, always exhibited a higher positive zeta potential than the other IONPs, which may be due to the binding of more number of lysozyme. This could be driven by the Na+ counterion induced electrostatic interaction at specific sites of the protein [20,21]. In other words, according to counterion induced interaction Model-II, the Na^+ counter ions released from STP-LMWC-IONPs will accumulate on the protein surfaces and then water molecules will diffuse the Na^+ counterions into protein hydrophobic core, thus leads to the unfolding of lysozyme [15]. As per the RCPC model, counterion-interacted lysozyme demonstrated a more positive zeta potential in pH 9.0 compared with pH 7.4. These results were further validated by comparison with the results from UV–visible, fluorescence and CD spectroscopy.

3.4. Investigating protein-nanoparticles interaction by UV–visible absorbance measurements

The UV–visible absorption band of lysozyme, in the range of 220–230 nm, was used to investigate any protein unfolding upon interaction with all the three types of NPs, at both the pH values (Fig. 4). The bands around 226 are attributed to the secondary folding of the protein and second band at 280 nm is due to the $\pi-\pi^*$ transition of aromatic amino acid residues (Tyrosine, Tryptophan and Phenylalanine), respectively [22].

After the interaction, an obvious decrease in the absorbance (at 226 nm) was observed with IONPs, LMWC-IONPs, and STP-LMWC-IONPs, at both pH 7.4 and 9.0 (Fig. 4A and B). The exact detectable changes (ΔA) at A_{226} were determined by subtracting the absorbance of 'native lysozyme' from the absorbance of 'interacted lysozyme', over the range of 220–250 nm, which showed the minima at around 226 nm. The decrease of ΔA at 226 nm, with a blue shift, is clearly observed upon interaction with STP-LMWC-IONPs; the ΔA being greater with all the IONPs at pH 9.0 than at pH 7.4 (shown in Fig. 4C and D). Using UV–vis absorption at 280 nm, the percentage of protein binding on the surface of NPs was calculated, by subtracting the unbound lysozyme present in the supernatant from the initial known concentration of lysozyme (see Fig. S1). These findings clearly indicated that pH 9.0 favors the strongest *reverse-charge-parity-counterion* (STP-LMWC-IONPs)

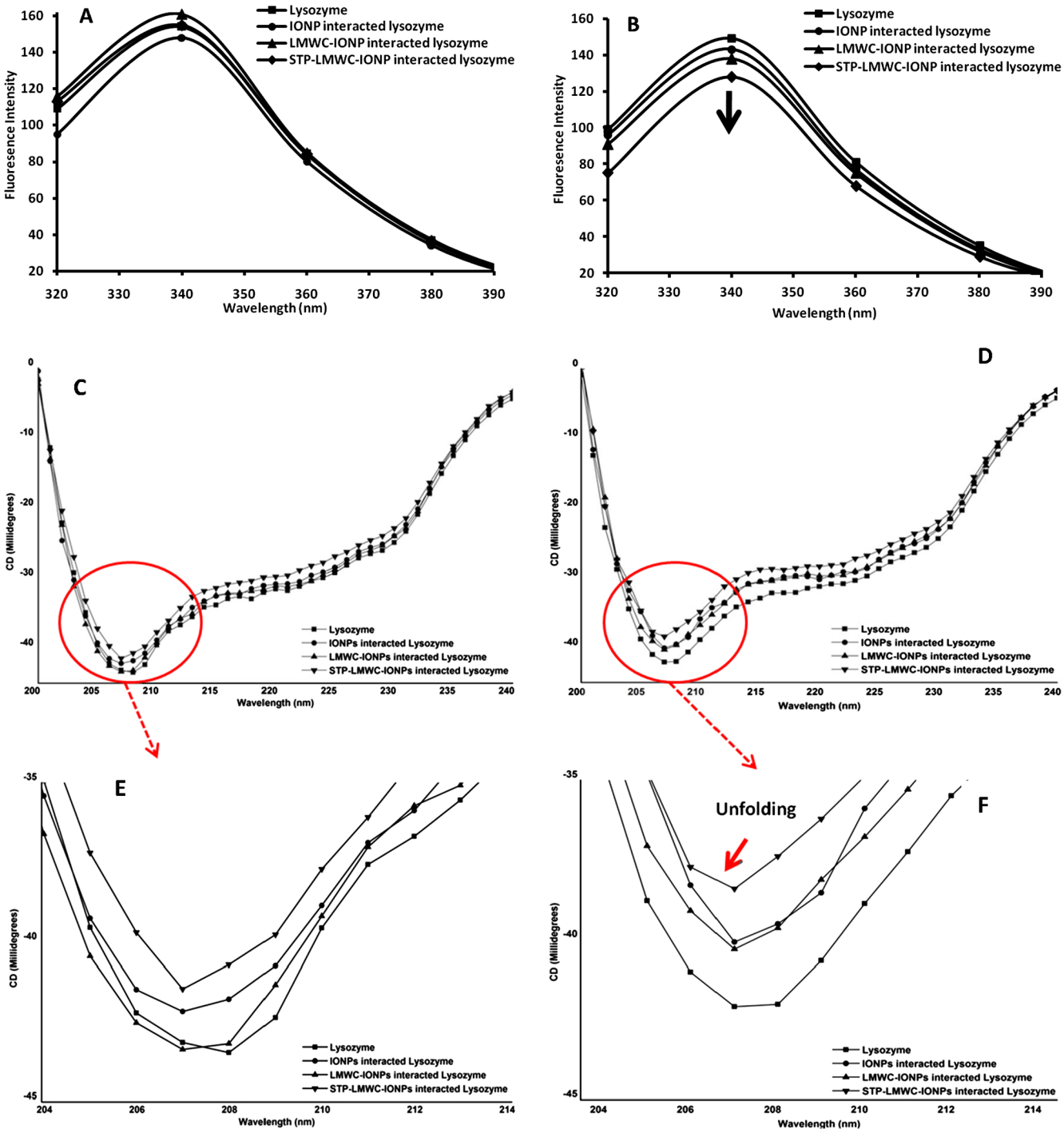

Fig. 5. Fluorescence quenching measurement of lysozyme, IONPs interacted lysozyme, LMWC-IONPs-Interacted lysozyme and STP-LMWC-IONPs-Interacted lysozyme at pH 7.4 (A) and 9.0 (B). CD spectra of lysozyme before and after interacting with NPs in pH 7.4 (C) and 9.0 (D). The E and F shows an expanded image of the C and D, respectively.

interaction with lysozyme. It further illustrated that the Na^+ counterions of STP play a crucial role in protein unfolding. The ΔA results are correlated well with those from our earlier report [23].

3.5. Fluorescence quenching measurements

The RCPC interaction of lysozyme with charged IONPs was further investigated by measuring the *quenching* of intrinsic fluorescence of tryptophan (Trp) residues of lysozyme, before and after interaction with bare and surface modified IONPs. The fluorescence band at 340 nm (upon excitation at 295 nm), showed any change in the band position in Fig. 5A (pH 7.4). The band corresponding to the IONPs-interacted lysozyme showed a slight decrease; whereas the band corresponding to the LMWC-IONPs interacted-lysozyme exhibited a slight increase in intensity. The increase in intensity was due to the lower negative charge on LMWC-IONPs that resulted in a weaker interaction with lysozyme. These results are consistent with the UV–visible results. Fig. 5B shows that the absorbance intensity gradually decreases after interaction with nanoparticles at pH 9.0. The findings are in good agreement with our earlier observations on fluorescence *quenching* of lysozyme upon IONPs

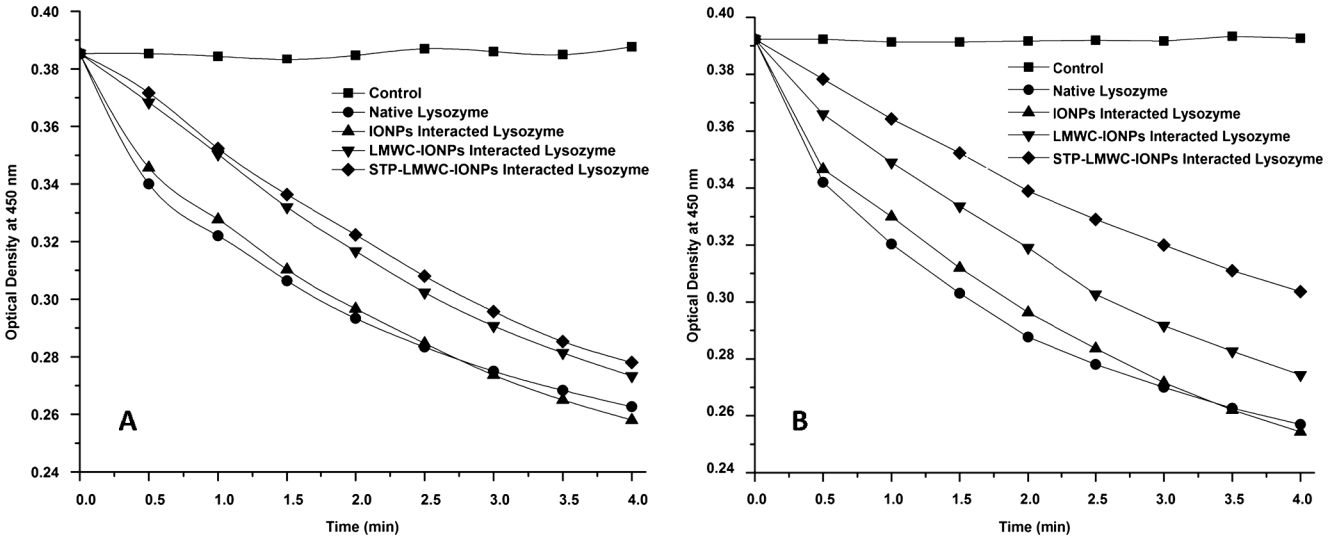

Fig. 6. Enzymatic activity of lysozyme, before and after interaction with NPs at pH 7.4 (A) and 9.0 (B).

interaction (in pH 9.0) [9]. The quenching order was observed as; IONPs < LMWC-IONPs ≪ STP-LMWC-IONPs at pH 9. The decrease in fluorescence intensity was assigned to the binding of Na^+ ions, as well as the complex formation of STP-LMWC-IONPs with Trp residues of lysozyme [15]. In addition, the increased negative surface charge of STP-LMWC-IONPs was thought to enhance the electrostatic binding with lysozyme, which resulted in a decrease in fluorescence intensity at pH 9.0.

3.6. Understanding the changes in secondary structure of the protein

Fig. 5C and D shows the CD spectra of lysozyme, before and after interacting with NPs, at pH 7.4 and pH 9.0, respectively. A small change in absorption minima of native lysozyme was observed with pH 9.0 due to the alteration in secondary structure or conformation of proteins, which are very sensitive to environmental factors such as pH and temperature. Upon NPs interaction at pH 9.0, the intensity of negative bands decreased remarkably, with a distinctive change in peak shape (see Fig. 5D), while the shape of the peaks and the peak position almost remains same at pH 7.4 (see Fig. 5C). Unfolding of secondary structure of lysozyme reduced (less negative) the CD spectra minimum at 208 nm, after interaction with charged nanoparticles [24,25]. This indicated the involvement of counterion binding with aromatic amino acid residues such as tyrosine, tryptophan, and phenylalanine. Compared to IONPs and LMWC-IONPs, the decrease in intensity was more in presence of counterion functionalized-IONPs (STP-LMWC-IONPs), at both pH 7.4 and 9.0, which could be due to the preferential binding of counterions (Na^+) with lysozyme *via* electrostatic interaction. This indicated an alteration in the secondary structural elements of lysozyme. According to RCPC model, pH 9.0 provides a suitable condition for the electrostatic interaction between lysozyme and STP-LMWC-IONPs. It is to be noted here that STP-LMWC-IONPs at pH 9.0 caused a remarkable reduction in the absorbance minima (CD signal intensity) compared with pH 7.4. These results indicated that the surrounding pH controlled the secondary folding of lysozyme during its interaction with IONPs. The findings are in good agreement with UV–visible results of our earlier publication [9]. These observations are also in compliance with the previous publication [15].

3.7. Enzymatic activity of nanoparticle-interacted lysozyme

The enzymatic activity can be directly correlated with the secondary folding of nanoparticle interacted-lysozyme, as shown in Fig. 6 since the activity of enzymes is solely dependent on their structural conformation [26]. In the active conformation of lysozyme the carboxyl groups of glutamic acid-35 (Glu 35) and the aspartic acid-52 (Asp 52) residues are the probable active binding sites for catalysis [27]. Both residues lie on opposite sides of a cleft in the surface of lysozyme, and are surrounded by a hydrophobic and hydrophilic environment, respectively. When both groups undergo complete ionization or protonation, the enzyme becomes inactive [28].

Fig. 6 shows the activity of nanoparticle interacted-lysozyme, in comparison to that with its native conformation, which indicated a decrease in the optical density (at 450 nm) of *M. lysodeikticus* cell suspension over time. Native lysozyme exhibited the highest enzymatic activity on *M. lysodeikticus* cells, at both, pH 7.4 and 9.0, which is in good agreement with an earlier report [28]. At pH 7.4 and 9.0, the enzymatic activity of lysozyme was gradually decreased with the conformational unfolding of lysozyme after the interaction.

It is worth noting that STP-LMWC-IONPs (counterion) interacted lysozyme showed a substantial decrease in activity at pH 9.0, than that of lysozyme interacted with IONPs and LMWC-IONPs. Clearly, the counterion induced inactivation of lysozyme can be observed at pH 9.0 (Fig. 6B). This may be attributed to the selective binding of Na^+ counterions with the glutamic acid-35 and the aspartic acid-52 amino acid residues, causing an unfolding in the lysozyme secondary confirmation at pH 9.0 [29,30]. The decrease in activity confirmed the ability of the counterion to unfold the native protein [31].

Fig. 7 shows microscopic images of lysozyme activity towards *M. lysodeikticus* cells, visualized by trypan blue staining under the microscope. Change in cell turbidity (aggregates) was observed visually after exposure to lysozyme. Fig. 7A and F show extreme turbidity of *M. lysodeikticus* cells (control) at pH 7.4 and 9.0, respectively, indicating the maximum number of organisms at these pH values. At both, pH 7.4 (Fig. 7B) and 9.0 (Fig. 7G), we found that the native lysozyme showed the maximum decrease in bacterial cell turbidity, as compared to the control. At both pH values, the reduction in cell turbidity gradually decreased depending on the enzymatic activity that solely depends on conformational unfolding. The incomplete degradation of bacterial cells indicates that lysozyme has lost its inherent cell lysis activity, upon interaction with nanoparticles and the reduction in activity was in the order, IONPs < LMWC-IONPs ≪ STP-LMWC-IONPs. Combined with CD and fluorescence data, counterion-induced change in secondary structure was accompanied with the inactivation of lysozyme lysing activity and a change in fluorescence intensity. This confirmed that the counterion-associated IONPs strongly interacted with lysozyme at pH 9.0 and that the secondary structure of the protein was affected by Na^+ counterions.

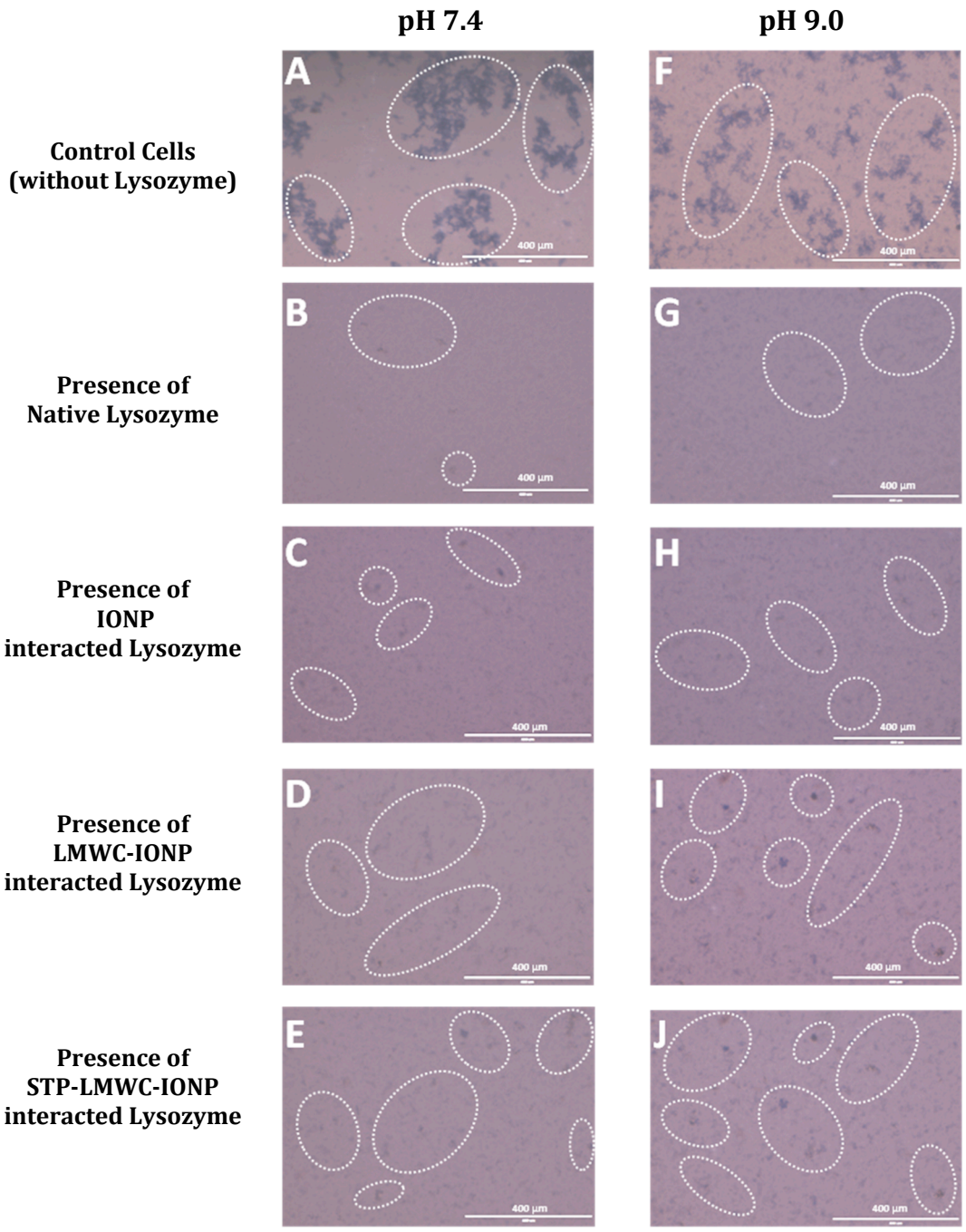

Fig. 7. Effect of nanoparticles on lysozyme activity towards *M. lysodeikticus* cells visualized by trypan blue staining under microscope, scale bar, 400 µm. Change in cells turbidity (aggregates) after exposure with native lysozyme (B), IONPs-Interacted lysozyme (C), LMWC-IONPs-Interacted lysozyme (D), STP-LMWC-IONPs-Interacted lysozyme (E) at pH 7.4. Similarly, native lysozyme (G), IONPs-Interacted lysozyme (H), LMWC-IONPs-Interacted lysozyme (I), STP-LMWC-IONPs-Interacted lysozyme (J) activity at pH 9.0. Image A and F shows only cells (control) at pH 7.4 and 9.0, respectively. Detected cells were marked with white colored dash circles.

4. Conclusion

In summary, *reverse-charge-parity-counterion* (RCPC) interaction of Na^+ associated STP-LMWC-IONPs with lysozyme was studied by UV–vis, fluorescence, and circular dichroism techniques at pH 7.4 and pH 9.0. Our results indicate that all three types of IONPs have ability to interact with lysozyme at both pH conditions. However, the counterions (Na^+) associated with STP-LMWC-IONPs showed selective binding with amino acids of lysozyme in pH 9.0, due to lysozyme-nanoparticle electrostatic interactions. Additionally, Na^+ counterions have a greater influence on the active sites of lysozyme and lead to a decrease in its lysing activity on *M. lysodeikticus* cells. Upon interaction with the counterion-associated STP-LMWC-IONPs, inactivation of lysozyme was also confirmed by the visual change in bacterial cell turbidity. At pH 9.0, counterion-induced conformational change (due to STP-LMWC-IONPs) and inactivation of lysozyme was more significant, than the bare IONPs and those without counterions (LMWC-IONPs). The effect of counterions during protein-nanoparticle electrostatic interaction (RCPC model) can be extended to other organic and inorganic nanoparticles and may be considered as an important indicator during the development of therapeutic nanomaterials.

Acknowledgements

This work was financially supported by UD/MUM/AO/CRS-M-213/2015 CSR, UGC-DAE Consortium for Scientific Research, Mumbai. The authors are thankful to BT/RLF/RE-ENTRY/51/2011-Ramalingaswami Fellowship, Department of biotechnology, India, SR/S2/RJN-139/2011-Ramanujan Fellowship, Department of science and technology, India and Department of Science and Technology (DST-Nanomission), Government of India (SR/S2/RJN-139/2011) for funding of Zetasizer. We are thankful to the NIRRH, Mumbai for allowing us access to the CD facility.

Conflict of interest

The authors have no conflicts of interest to declare.

Appendix A. Supplementary material

Supplementary data to this article can be found online at https://doi.org/10.1016/j.bioorg.2018.09.020.

References

[1] K. Siposova, K. Pospiskova, Z. Bednarikova, I. Safarik, M. Safarikova, M. Kubovcikova, P. Kopcansky, Z. Gazova, The molecular mass of dextran used to modify magnetite nanoparticles affects insulin amyloid aggregation, J. Magn. Magn. Mater. 427 (2017) 48–53.
[2] M. Zaman, E. Ahmad, A. Qadeer, G. Rabbani, R.H. Khan, Nanoparticles in relation to peptide and protein aggregation, Int. J. Nanomed. 9 (2014) 899.
[3] S. Ahmadian-Fard-Fini, M. Salavati-Niasari, H. Safardoust-Hojaghan, Hydrothermal green synthesis and photocatalytic activity of magnetic $CoFe_2O_4$–carbon quantum dots nanocomposite by turmeric precursor, J. Mater. Sci.: Mater. Electron. 28 (2017) 16205–16214.
[4] M. Suvarna, S. Dyawanapelly, B. Kansara, P. Dandekar, R.D. Jain, Understanding the stability of nanoparticle-proteins interactions: effect of particle size on adsorption, conformation and thermodynamic properties of serum albumin proteins, ACS Appl. Nano Mater. (2018), https://doi.org/10.1021/acsanm.1028b01019.
[5] A. Bellova, E. Bystrenova, M. Koneracka, P. Kopcansky, F. Valle, N. Tomasovicova, M. Timko, J. Bagelova, F. Biscarini, Z. Gazova, Effect of Fe_3O_4 magnetic nanoparticles on lysozyme amyloid aggregation, Nanotechnology 21 (2010) 065103.
[6] J. Xie, G. Liu, H.S. Eden, H. Ai, X. Chen, Surface-engineered magnetic nanoparticle platforms for cancer imaging and therapy, Acc. Chem. Res. 44 (2011) 883–892.
[7] M. Mahmoudi, H.R. Kalhor, S. Laurent, I. Lynch, Protein fibrillation and nanoparticle interactions: opportunities and challenges, Nanoscale 5 (2013) 2570–2588.
[8] S. Mirsadeghi, S. Shanehsazzadeh, F. Atyabi, R. Dinarvand, Effect of PEGylated superparamagnetic iron oxide nanoparticles (SPIONs) under magnetic field on amyloid beta fibrillation process, Mater. Sci. Eng., C 59 (2016) 390–397.
[9] S. Dyawanapelly, D.D. Jagtap, P. Dandekar, G. Ghosh, R. Jain, Assessing safety and protein interactions of surface-modified iron oxide nanoparticles for potential use in biomedical areas, Colloids Surf. B Biointerf. 154 (2017) 408–420.
[10] S. Dyawanapelly, U. Koli, V. Dharamdasani, R. Jain, P. Dandekar, Improved mucoadhesion and cell uptake of chitosan and chitosan oligosaccharide surface-modified polymer nanoparticles for mucosal delivery of proteins, Drug Deliv. Transl. Res. 6 (2016) 365–379.
[11] S. Poniková, A. Antošová, E. Demjén, D. Sedláková, J. Marek, R. Varhač, Z. Gažová, E. Sedlák, Lysozyme stability and amyloid fibrillization dependence on Hofmeister anions in acidic pH, J. Biol. Inorg. Chem. 20 (2015) 921–933.
[12] H.J. Zeng, M. Miao, R. Yang, L.B. Qu, Effect of silybin on the fibrillation of hen egg-white lysozyme, J. Mol. Recognit. 30 (2017).
[13] K. Das, K. Rawat, R. Patel, H. Bohidar, Size-dependent CdSe quantum dot–lysozyme interaction and effect on enzymatic activity, RSC Adv. 6 (2016) 46744–46754.
[14] G. Ghosh, L. Panicker, K. Barick, Selective binding of proteins on functional nanoparticles via reverse charge parity model: an in vitro study, Mater. Res. Express 1 (2014) 015017.
[15] G. Ghosh, L. Panicker, R. Ningthoujam, K. Barick, R. Tewari, Counter ion induced irreversible denaturation of hen egg white lysozyme upon electrostatic interaction with iron oxide nanoparticles: a predicted model, Colloids Surf. B Biointerf. 103 (2013) 267–274.
[16] M. Lucius, R. Falatach, C. McGlone, K. Makaroff, A. Danielson, C. Williams, J.C. Nix, D. Konkolewicz, R.C. Page, J.A. Berberich, Investigating the impact of polymer functional groups on the stability and activity of lysozyme-polymer conjugates, Biomacromolecules 17 (2016) 1123–1134.
[17] J. Nie, Z. Wang, K. Zhang, Q. Hu, Biomimetic multi-layered hollow chitosan–-tripolyphosphate rod with excellent mechanical performance, RSC Adv. 5 (2015) 37346–37352.
[18] G. Unsoy, S. Yalcin, R. Khodadust, G. Gunduz, U. Gunduz, Synthesis optimization and characterization of chitosan-coated iron oxide nanoparticles produced for biomedical applications, J. Nanoparticle Res. 14 (2012) 1–13.
[19] A.F. Martins, D.M. de Oliveira, A.G. Pereira, A.F. Rubira, E.C. Muniz, Chitosan/TPP microparticles obtained by microemulsion method applied in controlled release of heparin, Int. J. Biol. Macromol. 51 (2012) 1127–1133.
[20] S.R. Holbrook, S.M. Muskal, S.-H. Kim, Predicting surface exposure of amino acids from protein sequence, Protein Eng. 3 (1990) 659–665.
[21] W.-H. Lee, C.-Y. Loo, K.L. Van, A.V. Zavgorodniy, R. Rohanizadeh, Modulating protein adsorption onto hydroxyapatite particles using different amino acid treatments, J. R. Soc. Interf. 9 (2012) 918–927.
[22] C.B. Amara, N. Eghbal, P. Degraeve, A. Gharsallaoui, Using complex coacervation for lysozyme encapsulation by spray-drying, J. Food Eng. 183 (2016) 50–57.
[23] G. Ghosh, L. Panicker, K. Barick, Protein nanoparticle electrostatic interaction: size dependent counterions induced conformational change of hen egg white lysozyme, Colloids Surf. B Biointerf. 118 (2014) 1–6.
[24] K. Hemalatha, G. Madhumitha, N.A. Al-Dhabi, M.V. Arasu, Importance of fluorine in 2, 3-dihydroquinazolinone and its interaction study with lysozyme, J. Photochem. Photobiol., B 162 (2016) 176–188.
[25] Q. Li, T. Zhai, K. Du, Y. Li, W. Feng, Enzymatic activity regulated by a surfactant and hydroxypropyl β-cyclodextrin, Colloids Surf. B Biointerf. 112 (2013) 315–321.
[26] M. Liang, R. Liu, W. Qi, R. Su, Y. Yu, L. Wang, Z. He, Interaction between lysozyme and procyanidin: multilevel structural nature and effect of carbohydrates, Food Chem. 138 (2013) 1596–1603.
[27] N. Godjayev, S. Akyüz, L. Ismailova, The conformational properties of Glu 35 and Asp 52 of lysozyme active center, ARI-An Int. J. Phys. Eng. Sci. 51 (1998) 56–60.
[28] R. Davies, A. Neuberger, B. Wilson, The dependence of lysozyme activity on pH and ionic strength, Biochim. et Biophys. Acta (BBA)-Enzymol. 178 (1969) 294–305.
[29] S. Parsons, M. Raftery, Ionization behavior of the catalytic carboxyls of lysozyme. Effects of ionic strength, Biochemistry 11 (1972) 1623–1629.
[30] S. Gupta, S. Mahmood, R.H. Khan, A. Mahmood, Effect of Na+ ions on pH-dependent conformational changes in brush border sucrase-isomaltase in mice intestine, Indian J. Biochem. Biophys. 45 (2008) 399.
[31] S. Chaves, L.M. Pera, C.L. Avila, C.M. Romero, M. Baigori, F.E.M. Vieyra, C.D. Borsarelli, R.N. Chehin, Towards efficient biocatalysts: photo-immobilization of a lipase on novel lysozyme amyloid-like nanofibrils, RSC Adv. 6 (2016) 8528–8538.